UCPH NanoScience
NanoVidenskab KU

tidsskrift.dk/index.php/NanoVidenskabKU

Thesis Paper

Characterization of the formation of magic-sized $\{Bi_{38}O_{45}$ clusters by PDF and SAXS

Andy Sode Anker,*[a]

Submitted June 2018, accepted July 2018

Bismuth oxido clusters exist in a range of sizes, all built up by octahedral $\{Bi_6O_8\}$ units. While the atomic structure of various clusters has been solved by single crystal diffraction, it is much more challenging to study clusters directly in solution. Here, we use *in situ* X-ray total scattering with Pair Distribution Function (PDF) analysis to study the formation of the $\{Bi_{38}O_{45}\}$a cluster from $[Bi_6O_5(OH)_3(NO_3)_5]\cdot(H_2O)_3$ crystals dissolved in DMSO. The implementation of PDF analysis provides a unique insight into the structural rearrangements on the atomic scale. By combining with Small Angle X-ray Scattering (SAXS) we can furthermore investigate the size, morphology and size dispersion of the clusters taking place in the process. Consequently, the combination of these two complementary techniques provides a mean of bridging the local atomic and macroscopic characteristics of the material.

In the presented study, the results obtained show that the reaction goes through several stable intermediates before the magic-sized product $\{Bi_{38}O_{45}\}$ is reached. Through an associated temperature study, the intermediate was furthermore found to be capable of stabilization of up to days by varying the resulting reaction rate. The present studies show how powerful a tool the Debye Equation is in combination with SAXS and PDF, which in this field is a new development that has a large potential for unravelling important questions in nanochemistry in solution.

Introduction

In recent years, bismuth oxido clusters have been widely studied due to their applications ranging from medicin[1, 2], for designing radiopaque materials[2, 3] and building blocks for advanced catalysts[4], which all is possible due to their low toxicity[3, 5].

Bismuth oxido clusters exist in a range of sizes, all built up by octahedral $\{M_6O_X\}$ (M = Bi) units, which is commonly accepted as a building block in inorganic chemistry of large metal cations [6-8]. The octahedral $\{Bi_6O_8\}$ unit can be seen in Figure 1, right. With mass spectroscopy and single crystal diffraction, it has been shown that a range of large metal cations form stable clusters of $\{M_{22}O_X\}$ and $\{M_{38}O_X\}$[8-11] both built by octahedral $\{M_6O_X\}$ units. Both clusters are, for the bismuth oxido clusters, illustrated in Figure 2. The $\{M_{38}O_X\}$ cluster is sometimes referred to as magic-sized[8, 11], which means that they are atomically monodisperse[12].

Despite the large potential of using this as a model system in studies of fundamental cluster chemistry of large cations, the chemical processes involved in the cluster formation are not well understood[8], neither 22- or 38 bismuth atoms are equally dividable by 6, so how does the building blocks create the $\{Bi_{22}O_X\}$- and the $\{Bi_{38}O_{45}\}$ cluster?

While single crystal diffraction is restricted to samples of high crystallinity, it cannot be used to study materials in solution, as a result of the missing global order in the structure. Mass spectroscopy has been used to investigate the chemical composition of various clusters[13] but does not give any structural information. Therefore, it has been found challenging to study clusters directly in solution. This challenge can be generalized to other cluster systems[14].

If we were able to characterize the growth of the clusters on a molecular scale, we would get an understanding of the fundamental chemistry of clusters, and thereby be able to tailor-made materials with specific properties[8, 15]. This opens a new field of research, determining structures between molecules and particles[16, 17], whereas methods in the cross border of these fields must be used.

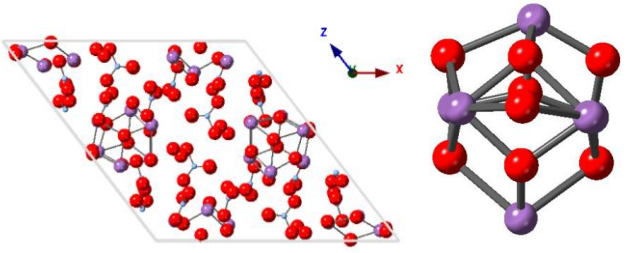

Figure 1: Left) The $[Bi_6O_5(OH)_3(NO_3)_5]\cdot(H_2O)_3$ crystal which is built by the Right) octahedral $\{Bi_6O_8\}$ unit. Purple) bismuth, red) oxygen, blue) nitrogen. Hydrogens are not included in the figure.

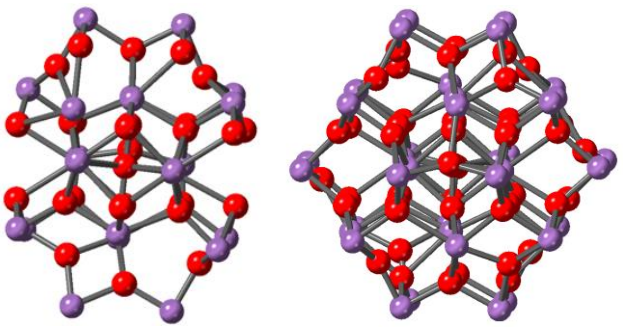

Figure 2: Left) The $\{Bi_{22}O_X\}$ cluster seen with single crystal diffraction and mass spectroscopy. Right) The $\{Bi_{38}O_{45}\}$ cluster seen with single crystal diffraction.

This study presents *in situ*[15] X-ray total scattering with Pair Distribution Function[14] (PDF) analysis of the formation of the $\{Bi_{38}O_{45}\}$ cluster in solution. $\{Bi_{38}O_{45}\}$ clusters are synthesized by dissolving crystals of $[Bi_6O_5(OH)_3(NO_3)_5]\cdot(H_2O)_3$ in DMSO.

The PDF analysis has given a unique insight into the structural rearrangements on an atomic scale, but PDF gives limited information on the nanometer scale. Therefore, Small-Angle X-ray Scattering[18] (SAXS) is used to investigate the size, morphology and size dispersion of the clusters taking place in the process. These two techniques complement each other allowing us to follow the cluster formation in both the local- and global order of the particle. The combination of SAXS and PDF bridge the local atomic and macroscopic characteristics of materials. Further work can be done in order to combine these techniques with complex modelling[19], which has a large potential for unravelling important questions in nanochemistry in solution[19, 20].

Since the bismuth oxido cluster does not consist of a periodic order, the Debye Scattering Equation[21, 22] is used to calculate the theoretical scattering. The Debye Equation is a sum of the scattering contribution from every atom in an isotropic sample which does not necessarily have to contain a periodicity in the structure.

Equation 1: $I(Q) = N_j {f_j}^2 + N_i {f_i}^2 + f_i f_j \sum_i^N \sum_{j\neq i}^N \frac{sin(Q\cdot r_{ij})}{Q\cdot r_{ij}}$

With the exponential increase in computational power the last decades[23], and the focus on nanomaterials, the Debye Scattering Equation becomes essential to characterize materials.

Further details of the methods are available in Supplementary S2.

Experimental section

Synthesis of $\{Bi_{38}O_{45}\}$ clusters for total scattering experiments

To characterize the formation of $\{Bi_{38}O_{45}\}$ clusters 131.4 mg of crystalline $[Bi_6O_5(OH)_3(NO_3)_5]\cdot(H_2O)_3$ was dissolved in 2 mL DMSO at room temperature. Additionally, a ligand exchange experiment was performed to investigate the effect of the ligand on the cluster structure. Therefore, 100 mg of $[Bi_{38}O_{45}(NO_3)_{24}(DMSO)_{25}]$ and 37 mg of $NaOOCC(CH_2)CH_3$ was dissolved in 2.5 mL DMSO. These solutions were used for *in situ* PDF[15] experiments at DESY, P02.1. The solutions were loaded in Kapton tubes with an inner diameter of 1.5 mm and measured at temperatures ranging from 30°C to 80°C with X-ray wavelength of 0.207170 Å.

In the *ex situ* PDF experiments, 32.85 mg of crystalline $[Bi_6O_5(OH)_3(NO_3)_5]\cdot(H_2O)_3$ was dissolved in 0.5 mL DMSO at room temperature and maintained undisturbed until measurements after 2 days, 4 days, 11 days and 100 days.

The experiments were performed at DESY, P07. The solutions were loaded in Kapton tubes with an inner diameter of 1.5 mm and measured at room temperature with X-ray wavelength of 0.123506 Å.

All total scattering data were integrated using the programme Fit2D[24], and Fourier transformed with PDFgetx3[25, 26] to obtain PDFs. The modelling was done using DiffPy-CMI[19]. When analysing the intermediate, only the bismuth atoms were modelled, since the radial distribution function is directly proportional to the form factor squared as well as the Debye Equation (Equation 1) (Supplementary S2.2.2).

Synthesis of $\{Bi_{38}O_{45}\}$ clusters for SAXS experiments

In the SAXS experiments 32.85 mg of crystalline $[Bi_6O_5(OH)_3(NO_3)_5]\cdot(H_2O)_3$ was dissolved in 0.5 mL DMSO at room temperature. Afterwards, the samples were stirred until no precipitate was left (a few hours) and maintained undisturbed until measurement after 5 hours and 45 hours.

Additionally, a sample was heated at 40°C, in order to investigate the kinetic behavior.

The SAXS experiments were done at the NBI Institute, Copenhagen. The solutions were loaded in glass capillaries tubes with an inner diameter of 0.6 mm and measured at room temperature with X-ray wavelength of 1.5418 Å.

The data were integrated using the programme Fit2D[24] and analyzed with SASfit[27] for the SAXS form factor analysis, and with a Python script for the calculations of the Debye equation (This is further elaborated in Supplementary S2.3.5).

Further details of the experiments are available in Supplementary S1, and details about the PDF- and SAXS analysis is in Supplementary S2.

Results and Discussion

Formation of the $\{Bi_{38}O_{45}\}$ cluster from the crystalline $[Bi_6O_5(OH)_3(NO_3)_5]\cdot(H_2O)_3$ dissolved in DMSO

Figure 3, left, shows the time-resolved PDFs obtained from the dissolution of $[Bi_6O_5(OH)_3(NO_3)_5]\cdot(H_2O)_3$ in DMSO at 80°C. The beginning of the reaction can from the long-range order be identified as a crystalline phase in suspension.

Figure 1, left, shows the crystalline $[Bi_6O_5(OH)_3(NO_3)_5]\cdot(H_2O)_3$ structure which was determined with single crystal diffraction[28] in 1978. It contains bismuth oxido clusters in the octahedral building block $\{Bi_6O_8\}$ as well as nitrate groups and water.

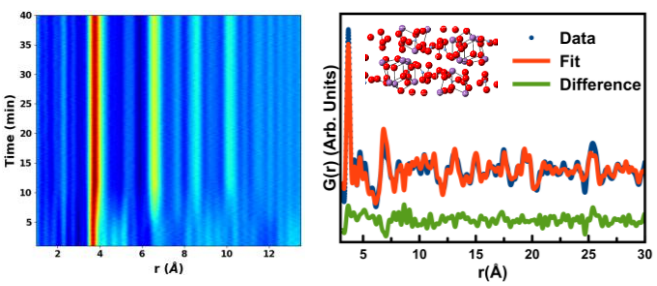

Figure 3: Left) The *in situ* measurement of the 80°C PDF measurement clearly indicates a structure change during the reaction. Right) The crystalline $[Bi_6O_5(OH)_3(NO_3)_5]\cdot(H_2O)_3$ phase describes the first 7 minutes of the reaction well. : Graph-description: Left) Time is plotted versus the interatomic distances in the cluster with the intensity shown with color code from light blue to dark red. Right) The probability of finding pairs of atoms separated by a distance "r" is plotted versus the interatomic distances, "r". R_w = 29.0 %.

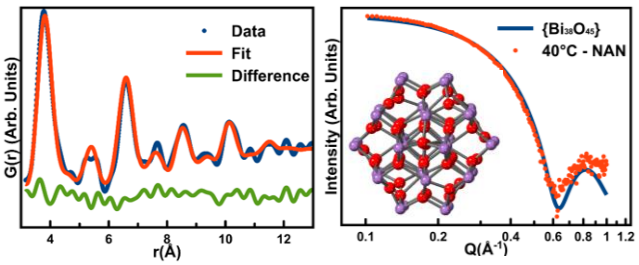

Figure 4: The last frames of the 80°C *in situ* PDF measurement are described well by the $\{Bi_{38}O_{45}\}$ structure. Left) The calculated structure of $\{Bi_{38}O_{45}\}$ with the Debye Equation describes the data after 40 minutes of the beginning of the experiment in the *in situ* PDF measurement well, right) The calculated structure of $\{Bi_{38}O_{45}\}$ with the Debye Equation describes the SAXS data from the sample prepared at 40°C well. Inset) The structure of $\{Bi_{38}O_{45}\}$. Graph-description: Right) The intensity is plotted versus the scattering vector **Q**.

At the beginning of the reaction, the PDFs can be fitted by the $Bi_6O_5(OH)_3(NO_3)_5]\cdot(H_2O)_3$ structure[28], as seen in Figure 3, right. Furthermore, a PDF was obtained by the crystalline $[Bi_6O_5(OH)_3(NO_3)_5]\cdot(H_2O)_3$ solid, which also fits well to the $[Bi_6O_5(OH)_3(NO_3)_5]\cdot(H_2O)_3$ structure from the literature (Supplementary S3.1.1 Figure 18). Since the molecular crystals have stronger intramolecular forces than intermolecular forces, the refinement was improved significantly by including two isotropic displacement factors[17] (Further details are available in Supplementary S3.1.2).

Within the first 7 minutes of the *in situ* PDF experiment performed at 80°C, the long-range order disappears as illustrated by the absence of the initial crystalline phase. This provides evidence of a structural change, where the crystalline suspension dissolves to small nanoparticles without long-range order.

At the last frame, which is 40 minutes after the beginning of the experiment, the reaction is expected to be in equilibrium and have formed $\{Bi_{38}O_{45}\}$, since a similar reaction has been seen to create $\{Bi_{38}O_{45}\}$ clusters[13]. This is furthermore confirmed by fitting a model of the calculated Debye Scattering from the $\{Bi_{38}O_{45}\}$ structure to the PDF from the last frame as seen in Figure 4, left.

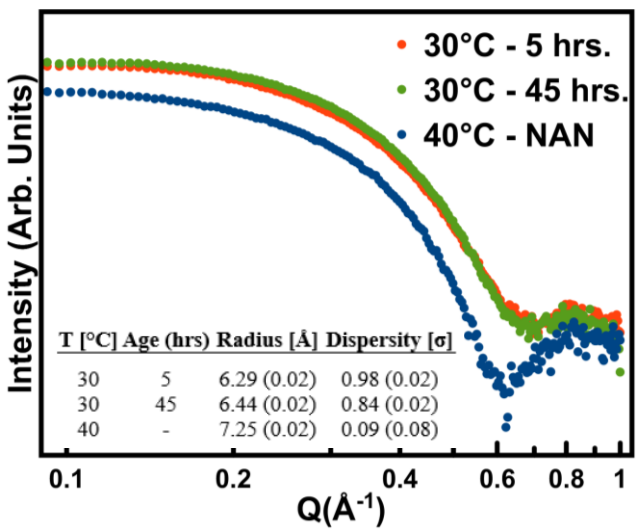

Figure 5: The SAXS measurements shows that the clusters will grow with time and temperature. Also the large cluster is characterized as magic-sized (fits are available in Supplementary S3.2.1).

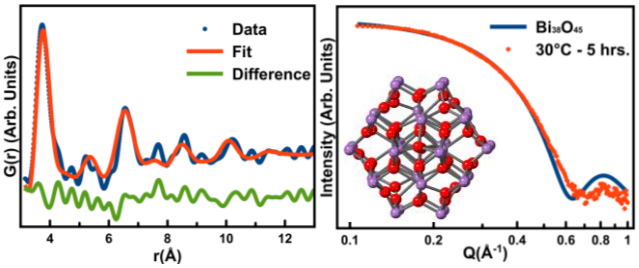

Figure 6: The data of the intermediate is not described well by the $\{Bi_{38}O_{45}\}$ structure. Left) The calculated structure of $\{Bi_{38}O_{45}\}$ with the Debye Equation does not describe the data of the 30°C *in situ* PDF measurement after 3 hours well. Right) The calculated structure of $\{Bi_{38}O_{45}\}$ with the Debye Equation does not describe the *ex situ* SAXS data of the 30°C measurement after 5 hours after the beginning of the experiment, well.

To support the *in situ* PDF data, *ex situ* SAXS data were obtained from samples prepared under similar conditions. Only the time and temperature of the reaction were different. Figure 4, right shows the Debye Scattering of the $\{Bi_{38}O_{45}\}$ structure fitted to the SAXS data of the sample prepared at 40°C. Since the model also describes the SAXS data very well, it indicates strongly that the dissolution of $[Bi_6O_5(OH)_3(NO_3)_5]\cdot(H_2O)_3$ in DMSO creates the $\{Bi_{38}O_{45}\}$ cluster at equilibrium. It has earlier been shown that similar reactions create stable $\{Bi_{38}O_{45}\}$ clusters[13] (Supplementary S3.6).

From an analysis of the SAXS form factor, the radius of the spherical $\{Bi_{38}O_{45}\}$ cluster was estimated to be 7.25 Å and the size dispersity to be 0.09 Å (Figure 5), which is the first time that it has been quantified that $\{Bi_{38}O_{45}\}$ is magic-sized in solution.

Investigating the PDF's obtained at lower temperatures, 30°C-60°C, the $\{Bi_{38}O_{45}\}$ cluster model does not describe the data well, indicating that the $\{Bi_{38}O_{45}\}$ cluster has not yet been formed. Figure 6, left, shows the calculated Debye scattering fitted to the *in situ* PDF measurement at 30°C after 3 hours of the experiment. The structure presented by the measured data does exhibit similarities to the utilized $\{Bi_{38}O_{45}\}$ cluster model. However, for a few of the peaks, such as at r = 7.8 Å, the intensity is not fully described with the given model. Concludingly, the given structure must be described as a structure with some similar structural features of the known $\{Bi_{38}O_{45}\}$ structure, but it cannot solely be described with this model. Furthermore, *ex situ* SAXS data of the sample prepared at room temperature and measured 5 hours after initialization of the experiment was modelled with the $\{Bi_{38}O_{45}\}$ cluster in Figure 6, right. It can be seen that the model in the high Q-value regime does not fit the data well, which supports the conclusion that this is an intermediate. Both the PDF and SAXS data collected from samples prepared at low temperatures cannot

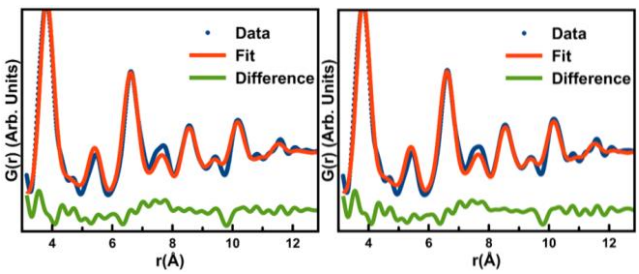

Figure 7: The $\{Bi_{38}O_{45}\}$ structure describes the *ex situ* PDF data of the samples prepared at room temperature well after – left) 2 days, right) 100 days.

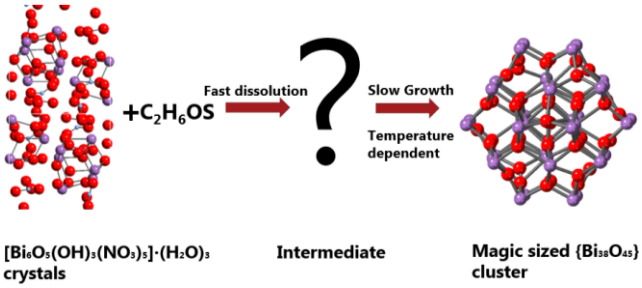

Figure 8: The $[Bi_6O_5(OH)_3(NO_3)_5]\bullet(H_2O)_3$ crystals dissolved in DMSO have shown to go through an intermediate before growing to a magic-sized $\{Bi_{38}O_{45}\}$ cluster.

be described with the $\{Bi_{38}O_{45}\}$ cluster model, which is identified by the poor fits obtained. The full analysis can be read in Supplementary S3.1.4.

Ex situ measurements of samples prepared at room temperature were done to characterize the reaction after 2 days, 4 days, 11 days and 100 days, which are illustrated in Figure 7. The structures of all of these samples correspond to $\{Bi_{38}O_{45}\}$ (Supplementary S3.1.4). Therefore, the equilibrium of the reaction seems to go towards $\{Bi_{38}O_{45}\}$ but is both temperature dependent and time-dependent. At 80°C, the reaction goes to equilibrium in minutes, where it takes days at room temperature.

Analysis of intermediate structures

As presented above, it has been established that the first 7 minutes of the *in situ* PDF measurement at 80°C in Figure 3, left, corresponds to the crystalline phase of $[Bi_6O_5(OH)_3(NO_3)_5]\cdot(H_2O)_3$ and the frames after 40 minutes corresponds to the $\{Bi_{38}O_{45}\}$ cluster. Figure 8 illustrates the reaction pathway, in which the intermediate structure is still to be elucidated. This is supported by Figure 9, which shows that the middle frame and last frame are not the same.

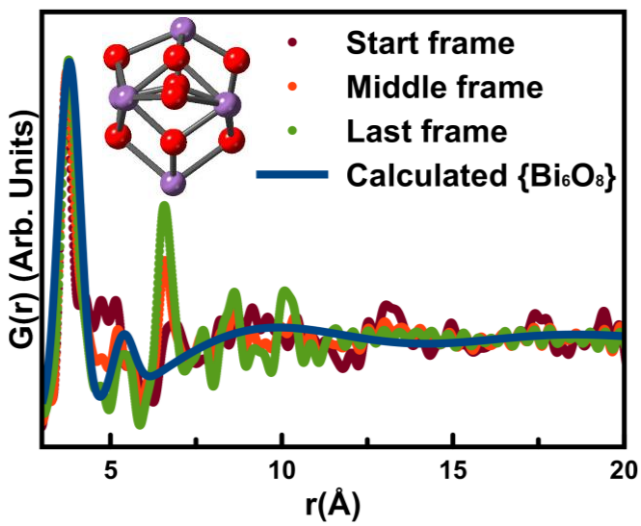

Figure 9: Data from frames through the reaction compared to the calculated structure of the octahedral $\{Bi_6O_8\}$ unit, which shows that the octahedral $\{Bi_6O_8\}$ unit is not stable in solution. Inset: The structure of the octahedral $\{Bi_6O_8\}$ unit.

[1] Troels Lindahl Christiansen found that the octahedral building block octahedral $\{M_6O_X\}$ was never stable in solution.

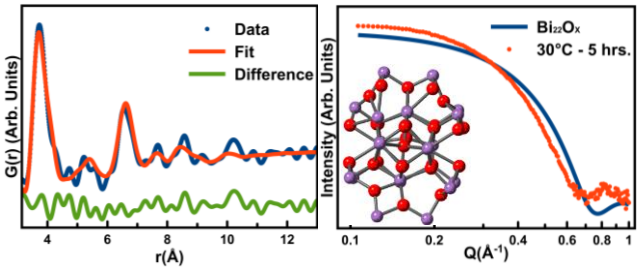

Figure 10: The frames corresponding to the intermediate structure in the *in situ* PDF measurement is not described well by the $\{Bi_{22}O_X\}$ structure. Left) The calculated structure of $\{Bi_{22}O_X\}$ with the Debye Equation fit the data of the frames after 3 hours after the beginning of the experiment of the 30°C *in situ* measurement partially, right) The calculated structure of $\{Bi_{22}O_X\}$ with the Debye Equation fitted to the SAXS data from the sample prepared at 30°C after 5 hours. Inset) The structure of $\{Bi_{22}O_X\}$. Refined parameters can be seen in Supplementary S3.1.4.

But from the *in situ* PDF measurement in Figure 3, left, it seems like the crystalline phase dissolves into an intermediate, before the formation of $\{Bi_{38}O_{45}\}$. When the long-range order disappears after 7 minutes, the peaks at r = 3.8 Å, r = 6.3 Å, r = 8.2 Å and r = 10.2 Å increases in intensity until it is similar to the $\{Bi_{38}O_{45}\}$ cluster. This must represent the intermediate, which is assumed to be the same structure in all experiments despite the varying temperature (Figure 6 + Figure 17).

Since the octahedral building block, $\{Bi_6O_8\}$, is referred to as particularly stable in the literature[6-8], it is expected that the crystals will dissolve into clusters of building blocks with nitrate functioning as ligands. By comparing the calculated PDF of the octahedral building block $\{Bi_6O_8\}$ with an early frame, a middle frame and the last frame of the 80°C *in situ* PDF data, it can be seen that $\{Bi_6O_8\}$ is never stable in solution[1] (Figure 9), since the structure of the presented data contains distances significantly longer than the octahedral $\{Bi_6O_8\}$ does.

From Figure 9 it can clearly be seen that the middle frame and last frame are different, especially in the peak at r = 6.5 Å, which is an intermolecular distance between two $\{Bi_6O_8\}$ building blocks. Therefore, the intermediate must be a smaller cluster than the product. This agrees with what is chemically expected as we have a cluster growth proceeding in the reaction. Cluster Growth is furthermore verified through analysis of the SAXS form factor in Figure 5 since the particles prepared at 30°C and measured after 5 hours has a radius of 6.25 Å, which is smaller than the $\{Bi_{38}O_{45}\}$ cluster with a radius of 7.25 Å.

While the octahedral building block, $\{Bi_6O_8\}$, is not seen stable in solution, it is instead utilized to build an intermediate structure. A similar structure composed of 22 bismuth atoms as the one presented in Figure 2, left, has been identified with single crystal diffraction[29]. Additionally, based on mass spectroscopy, a cluster of 22 bismuth atoms has been observed from a similar reaction[13]. Therefore, a $\{Bi_{22}O_X\}$ structure was built simply by putting the $\{Bi_6O_8\}$ units together, which can be seen in Figure 2, left. In Figure 2, it is seen that the $\{Bi_{22}O_X\}$ structure is similar to the $\{Bi_{38}O_{45}\}$ structure, both built by the octahedral building blocks,

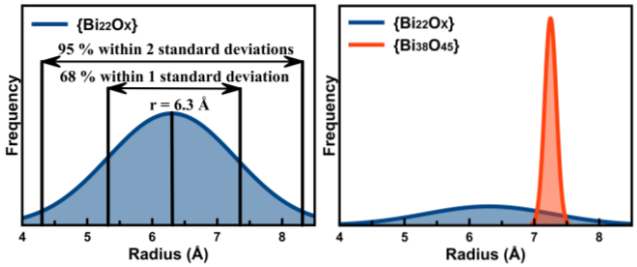

Figure 11: The size distributions of the clusters found with SAXS form factor analysis of the SAXS data of the sample prepared at 30°C and measured after 5 hours after the beginning of the experiment and the sample prepared at 40°C. Left) The size distribution of the intermediate, $\{Bi_{22}O_X\}$ cluster. Right) The comparison of the size distributions of the intermediate, $\{Bi_{22}O_X\}$, and the product, $\{Bi_{38}O_{45}\}$.

$\{Bi_6O_8\}$, but the two clusters are different in size. Afterwards, the constructed $\{Bi_{22}O_X\}$ cluster was fitted to the data from the intermediate. However, as observed in Figure 10, the data is only partially described, with good agreement between the peaks at r = 3.8 Å and r = 6.3 Å, while the smaller peaks at r = 8.2 Å and r = 10.2 Å cannot be fully described with the current model.

Apart from the cluster growth indications provided through the SAXS measurements, the measurements furthermore displayed a larger size distribution (0.94 Å) than in the final product as illustrated in Figure 5. Eventually, this indicates that the intermediate is disordered. The SAXS form factor analysis has been done by fitting a spherical SAXS form factor with a Gaussian curve to the data. Thereby, a size distribution of clusters can be illustrated as seen in Figure 11. Here the frequency of clusters with radius "R" is plotted versus the radius "R". In Figure 11, left, it can be seen that 68 % of the clusters in the intermediate has a radius in range R = 5.3 Å – 7.3 Å, while this is compared to the $\{Bi_{38}O_{45}\}$ cluster in Figure 11, right, where 68 % of the clusters has a radius of R = 7.16 Å – 7.34 Å.

These results indicate that the reaction goes through a spherical polydisperse intermediate before growing to the spherical magic-sized $\{Bi_{38}O_{45}\}$ cluster (further analysis and results of the SAXS data can be found in Supplementary S3.2.1).

Based upon the above-stated results, it has been shown that all the clusters are build up by the octahedral building block, $\{Bi_6O_8\}$, and that the product is the well-defined structure of $\{Bi_{38}O_{45}\}$.

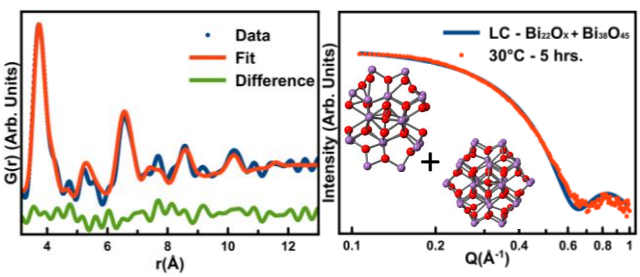

Figure 12: Data corresponding to the intermediate in the *in situ* PDF measurement is described well by a linear combination of the $\{Bi_{38}O_{45}\}$ cluster and the $\{Bi_{22}O_X\}$ cluster. Left) The calculated structure of a linear combination of the calculated Debye scattering of the $\{Bi_{38}O_{45}\}$ and the $\{Bi_{22}O_X\}$ describes the data of the frames after 3 hours from the beginning of the experiment of the 30°C *in situ* PDF measurement well, right) The calculated structure of a linear combination of the calculated Debye scattering of the $\{Bi_{38}O_{45}\}$ and the $\{Bi_{22}O_X\}$ describes the SAXS data from the sample prepared at 30°C after 5 hours well. Inset) The linear combination of the $\{Bi_{22}O_X\}$ and the $\{Bi_{38}O_{45}\}$ cluster.

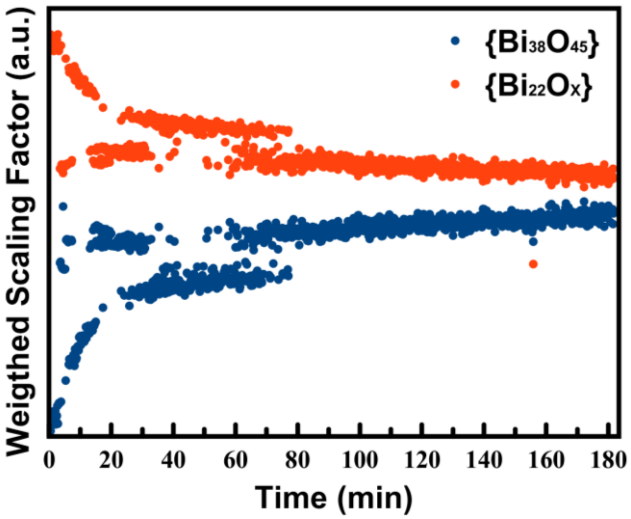

Figure 13: The scaling factor versus time of the reaction from the beginning of the experiment is plotted from the 30°C *in situ* PDF measurement, which shows that the $\{Bi_{22}O_X\}$ cluster is growing to the $\{Bi_{38}O_{45}\}$ cluster.

On the search for a complete solution; introducing a multi-phase refinement

From the previous investigations, it was found that single-phase refinement with either the $\{Bi_{22}O_X\}$- or $\{Bi_{38}O_{45}\}$ cluster as the model did provide a description of some structural features, but still with severe discrepancies between model and experimental data. Therefore, it was motivated to investigate if the reaction instead should be considered as consisting of two phases, the $\{Bi_{22}O_X\}$- and $\{Bi_{38}O_{45}\}$ cluster. Consequently, a two-phase refinement was performed on both the PDF and SAXS data. When a linear combination of the calculated Debye scattering from the $\{Bi_{22}O_X\}$ cluster and the $\{Bi_{38}O_{45}\}$ cluster is fitted to the 30°C *in situ* PDF data after 3 hours, and subsequently to the SAXS data which were prepared at low temperature, it can be seen that they describe the data very well (Figure 12). The SAXS form factor analysis can equally well be described by a two-phase refinement of magic-sized structures, with similar dimensions as the $\{Bi_{22}O_X\}$ cluster and the $\{Bi_{38}O_{45}\}$ cluster, as a polydisperse intermediate (Further details are available in Supplementary S3.2.1). Sequential refinement was done on the *in situ* PDF data, where the weighted scaling factor of the individual clusters can be seen as an indicator of how much the cluster is present in the sample (Further details in Supplementary S3.4). In Figure 13, it can be seen that the weighted scaling factors of the two clusters are changing through the reaction. The reaction can, in the beginning, be described as a large fraction of the $\{Bi_{22}O_X\}$ cluster and small amounts of $\{Bi_{38}O_{45}\}$, but with time the $\{Bi_{38}O_{45}\}$ cluster becomes more dominant. In Figure 14 the ratio between the two clusters is plotted versus the time after the beginning of the experiment. High values mean a high ratio of the $\{Bi_{22}O_X\}$ cluster, and low values mean a high ratio of the $\{Bi_{38}O_{45}\}$ cluster. It can be seen that the reaction can be divided into two regions; at the beginning of the reaction, the cluster ratio rapidly changes, which is followed by a rather constant change in cluster ratio throughout the reaction. Furthermore, as illustrated in Figure 14, the temperature is also observed to have an effect on the reaction rate and therefore dictates how rapid the reaction is growing from the intermediate to the $\{Bi_{38}O_{45}\}$ cluster.

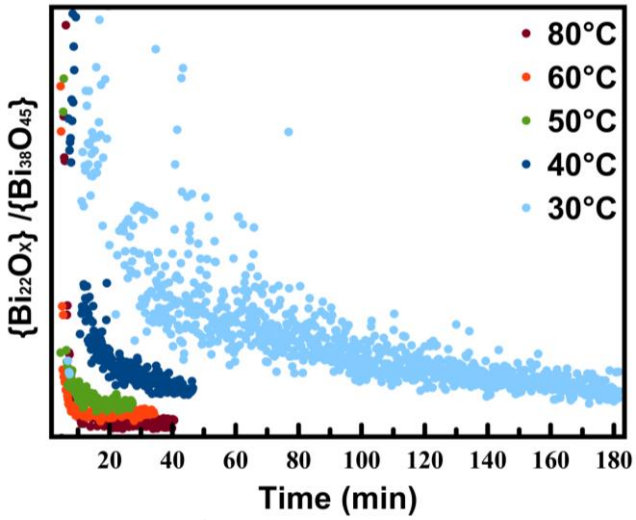

Figure 14: The ratio of $\{Bi_{22}O_X\}$ cluster and $\{Bi_{38}O_{45}\}$ cluster is plotted versus time of the reaction. It can be seen that the intermediate is growing until it becomes the $\{Bi_{38}O_{45}\}$ cluster. The rate of ratio change is highly temperature- and time-dependent.

How fast the conversion occurs between the $\{Bi_{22}O_X\}$- and $\{Bi_{38}O_{45}\}$ cluster has been further investigated through *ex situ* PDF measurements.

The data were measured at 30°C after 2 days, 4 days, 11 days and 100 days. By introducing the two-phase model for refinement, the resulting fit was significantly improved (Figure 15).

Furthermore, it can be seen that the ratio between the $\{Bi_{22}O_X\}$ - and $\{Bi_{38}O_{45}\}$ cluster is lower than for the high temperature *in situ* PDF measurements for 40 minutes (Supplementary S3.4), which indicates that both the time dependency and temperature dependency have a significant effect.

This conventional modelling technique, which has so far been introduced, provides a reasonable idea of the overall cluster growth process, where the intermediate is growing until it becomes the $\{Bi_{38}O_{45}\}$ cluster. However, limited insight can be achieved, when considering how the cluster growth is happening. To gain such information, a new approach must be introduced.

Predicting the average structure through computational permutations

A new way of modelling the PDF data is introduced in order to characterize the average structure through the reaction. All possible models, with the same motif as the $\{Bi_{22}O_X\}$- and the $\{Bi_{38}O_{45}\}$ cluster must be tried in order to eventually obtain the best possible structure (Supplementary S3.3 Figure 37).

The procedure of this approach is initialized by fitting a structure

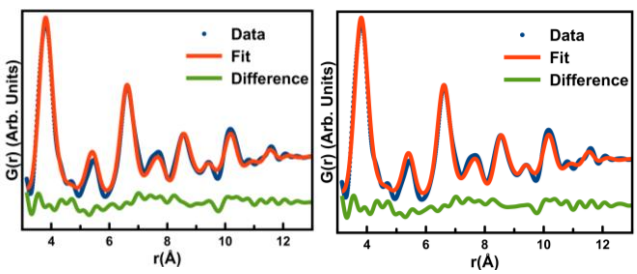

Figure 15: The linear combination of the $\{Bi_{22}O_X\}$ cluster and $\{Bi_{38}O_{45}\}$ cluster describes the *ex situ* data of the samples well after – left) 2 days, right) 100 days.

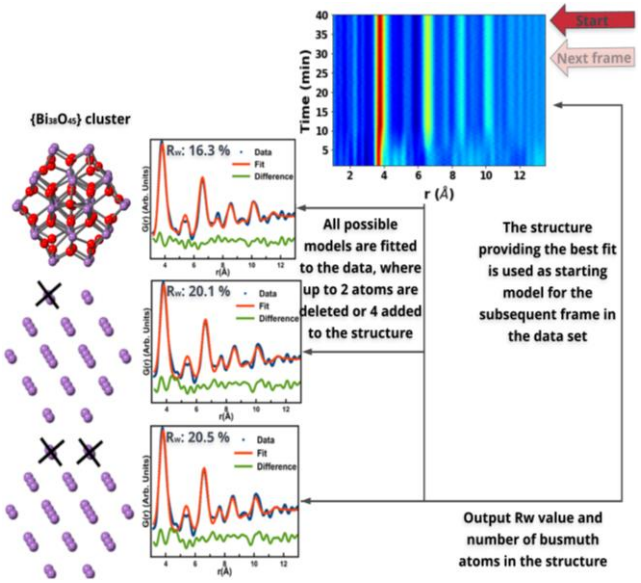

Figure 16: The permutations method follows the steps:

1. Fit the data of the last frame to all permutated structures of the $\{Bi_{38}O_{45}\}$ cluster.
2. Output the structure which describes the last frame best.
3. Go 1 frame backwards and fit the data to all permutated structures derived from the outputted structure.
4. Output the structure which describes the data of the second to last frame best.

to a frame of the *in situ* PDF measurement. Proceeding from this, atoms are added or deleted to the structure individually in order to find a structure, which describes the data better. When the best possible structure is found, this is used as a starting point for the next frame, where atoms are deleted or added again. (Full description of this modelling method is available in Supplementary 2.4 & 3.3).

Be aware that the method can only be used when the structural motif is the same through the reaction, in which only the size of the cluster may vary.

The reaction can be followed by starting from the product and using this method backwards in the reaction by deleting atoms or adding atoms to the structure in order to find the structure, which describes the data best. This method is illustrated by a flowchart in Figure 16.

To avoid the unphysical values, the method was restricted. The cluster cannot contain more than 38 bismuth atoms and it cannot be smaller than the octahedral building block. Only one larger cluster is reported in the literature $[Bi_{50}Na_2O_{64}(OH)_2(OSiMe)_3)_{22}]$[30], which does not fit the data well (Supplementary S3.5). The correlated motion, delta2, was restrained to between 0 and 7, the zoomscale between 0.9 and 1.1 and the atomic displacement parameter should be between 0 and 3.

Permutations are done by adding 2 atoms per frame, which were the most inner atoms of the ones missing and deleting up to 6 atoms, which were always from the outer sphere of the particle. Ideally, all 38 bismuth atoms had to be included in the permutations, but this gives 2^{38} structures that have to be fitted to the data. Due to limited computational power, this is not possible. By experience, it was seen that 6 atoms are sufficient to follow the reaction process when 1 frame corresponds to 4 seconds.

Figure 17 shows the results of the time-resolved permutation. The

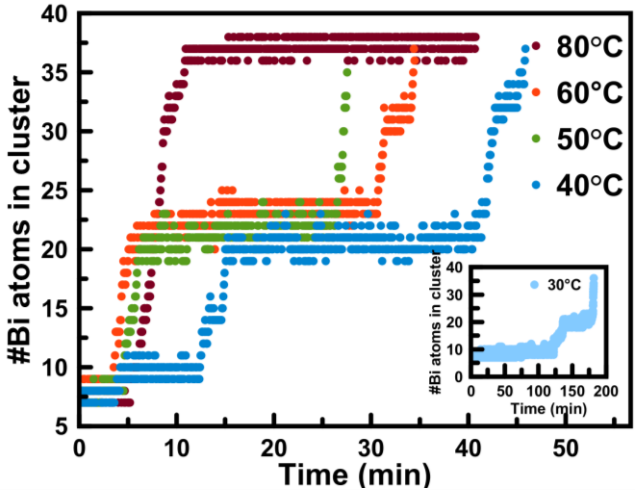

Figure 17: The reaction goes through several intermediates, which's stability is dependent of the temperature, before ending as the $\{Bi_{38}O_{45}\}$ cluster. Graph-description: The number of bismuth atoms in the best possible structure of the frame is plotted versus reaction time.

number of bismuth atoms is plotted versus the time of the reaction; thus a reaction process of the average structure in the sample is shown. It is evident that the reaction goes through multiple intermediates.

From Figure 17, it is seen that an intermediate of 19-23 bismuth atoms appears, which upon both lower temperatures and longer reaction-time, grows to an intermediate of 30-34 bismuth atoms before the stable $\{Bi_{38}O_{45}\}$ structure is seen. Both intermediates are only stable with low temperature and the $\{Bi_{38}O_{45}\}$ cluster is only seen at 80°C. Furthermore, the 30-34 bismuth intermediate is only seen at measurements longer than 30 minutes (Figure 17). In order to confirm the results, the residuals and the physical structure of every frame can be shown by this method. In Figure 18, left, the residuals are shown as function of the number of bismuth atoms in the structure. It can be seen that all intermediate states before the 19-23 atom intermediate have a high R_w value. In Figure 18, right, a selected structure with less than 19 bismuth atoms is illustrated. This illustrates that when the structures have less than 19 atoms, they are seen to be unphysical and fit the data with high R_w values, which probably are caused by some crystalline material in the sample.

In Figure 19, left, all structures larger than 19 bismuth atoms are plotted as function of how frequent they appear. In Figure 19, right, the most frequent structures through the reaction are shown. They

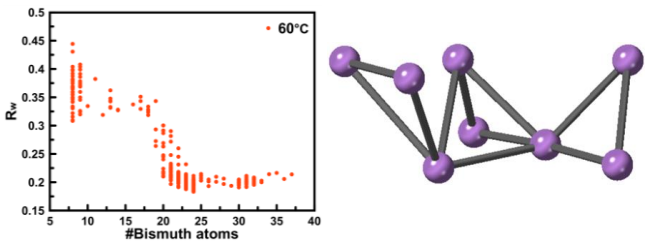

Figure 18: Left) The R_W values plotted against the number of bismuth atoms in the best possible structure of the frame. Right) One of the structures with high R_W value, which shows that these frames in the beginning of the reaction does not give a physical output.

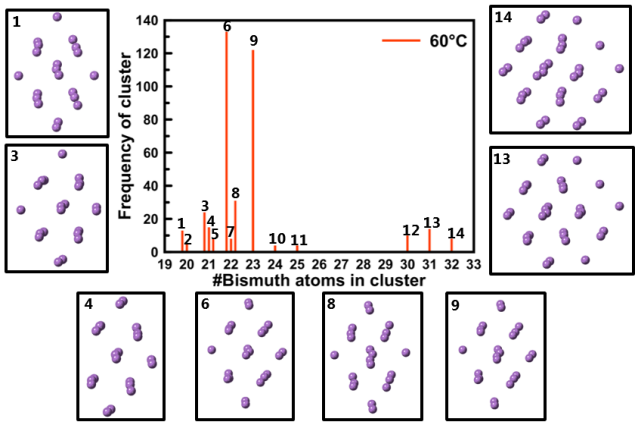

Figure 19: Left) The frequency of the clusters are plotted versus how many bismuth atoms they contain. Boxes) Illustrates which structures the reaction goes through.

all seem physical and consisting of the octahedral building block, $\{Bi_6O_8\}$.

For the 60°C *in situ* PDF measurement, the intermediate structures that were made this way by deleting atoms from the $\{Bi_{38}O_{45}\}$ structure, were investigated. 14 different structures were found between the crystalline phase and the $\{Bi_{38}O_{45}\}$ structure (Figure 19), where the most frequent structures are denoted as number 6 and 9 (Further analysis of the intermediates of the 30°C *in situ* PDF measurement are available in Supplementary S3.3.1.1). It is also showed that the PDF's cannot distinguish all these structures, but they are all physical following the building block principle (Supplementary S3.3.1 figure 38).

It can be seen that characterization of the cluster formation is very complex. Traditional refinements only show that the cluster is growing, but does not tell anything about how it is growing. Therefore, a new modelling technique was designed, where the structure was permuted. This means that the model is chosen relative to the earlier frame. With this technique, the average cluster growth process has been characterized. Both techniques are essential in order to understand the reaction process (Further comparison of the two techniques are available in Supplementary S3.8).

Exchange of ligands from $[Bi_{38}O_{45}(NO_3)_{24}(DMSO)_{25}]$ to $[Bi_{38}O_{45}(OMc)_{24}(DMSO)_{25}]$

In order to control the synthesis, one must not only be able to control the synthesis with nitrate as a ligand, but with all kind of ligands. To characterize the effect of the ligand, a replacement of the nitrate ligand with $NaOOC(CH_2)CH_3$ was measured *in situ* (Figure 20) at 30°C.

It is evident that changing the ligand directly changes the structure of the bismuth clusters in the reaction[2]. Comparing the first frame after dissolution and the last frame of the 30°C *in situ* ligand exchange PDF measurement with the $\{Bi_{38}O_{45}\}$ cluster reveals that the model describes the data reasonably just after dissolution, which is 5 minutes after the beginning of the experiment. However, following the introduction of ligand exchange, the fit is significantly improved, showing good agreement between data and

[2] I want to credit Troels Lindahl Christiansen for making this observation

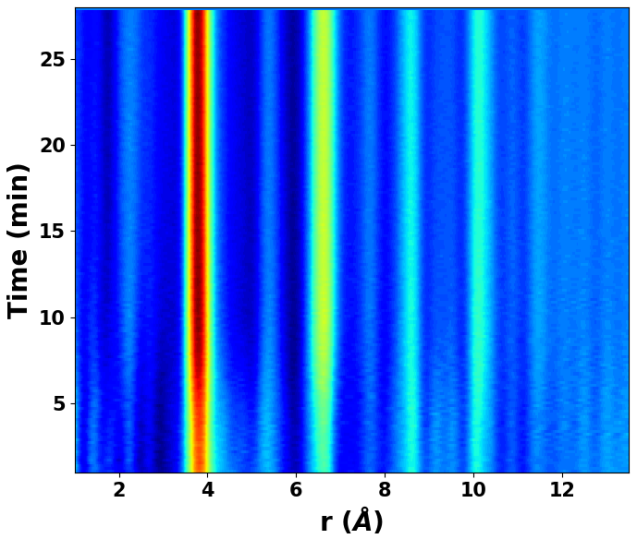

Figure 20: The 30°C *in situ* PDF measurement of the ligand exchange experiment clearly indicates a structure change during the reaction.

the utilized $\{Bi_{38}O_{45}\}$ cluster model. Consequently, this indicates that $NaOOC(CH_2)CH_3$ is found to stabilize the core built by the building blocks (Figure 21) (Further details is available in Supplementary S3.7).

However, the reasoning of why this ligand has a stabilizing effect is yet unknown, but interesting it is that the ligand has such a great effect on the structure of the clusters. Additionally, for further studies, it would be interesting to use $NaOOC(CH_2)CH_3$ in the cluster growth process to investigate if the intermediates could be further stabilized.

The full analysis is available in Supplementary S3 with a description of the individual contributions from Troels Lindahl Christiansen, Martin Schmiele and Andy Sode Anker.

Conclusion

The experiments reported here demonstrate how challenging it is to characterize clusters directly in solution. Meanwhile, it has been demonstrated how powerful a tool the Debye Equation is, and how it can be used with both PDF and SAXS to characterize complex systems of multiple phases and size distributions of structures. The combination of PDF and SAXS has shown its large potential in material chemistry of nanomaterials.

In the presented study, crystalline $[Bi_6O_5(OH)_3(NO_3)_5]\cdot(H_2O)_3$ was dissolved in DMSO, in which it was found that the material directly forms into a bismuth oxido cluster containing about 22

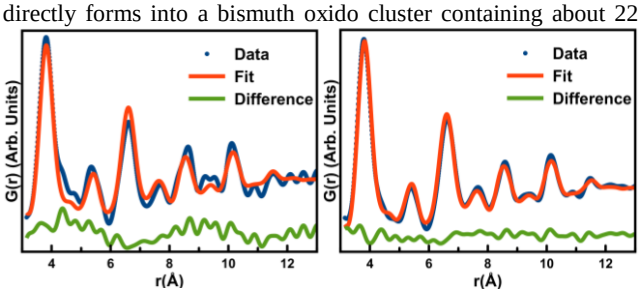

Figure 21: Left: The first frame after dissolution of the *in situ* PDF measurement of the ligand exchange fitted to the $\{Bi_{38}O_{45}\}$ cluster. Right: The last frame, which corresponds to 29 minutes after beginning of the experiment, fitted to the $\{Bi_{38}O_{45}\}$ cluster.

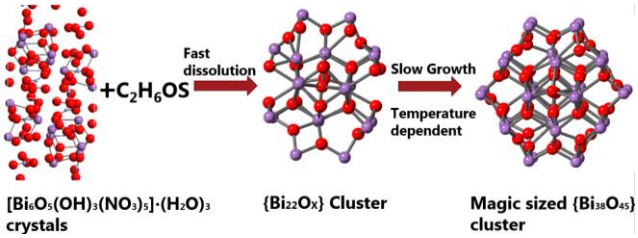

Figure 22: The $[Bi_6O_5(OH)_3(NO_3)_5]\bullet(H_2O)_3$ crystals dissolved in DMSO have shown to go through an $\{Bi_{22}O_X\}$ cluster as intermediate before growing to a magic-sized $\{Bi_{38}O_{45}\}$ cluster.

bismuth atoms, but not through a stable octahedral $\{Bi_6O_8\}$ unit as assumed in earlier studies[13]. The product was characterized as the atomically stable $\{Bi_{38}O_{45}\}$ compound, which could be further stabilized by varying the ligand. It is the first time that it has been quantified that the $\{Bi_{38}O_{45}\}$ structure is magic-sized in solution. In order to characterize the intermediate two modelling approaches were used. The traditional PDF methods were used with a two-phase refinement to follow the reaction process from the $\{Bi_{22}O_X\}$ cluster to the $\{Bi_{38}O_{45}\}$ cluster. This method showed that the intermediate was found to grow until it reached the $\{Bi_{38}O_{45}\}$ cluster. However, the current method does not provide any additional information regarding the unique structure(s) through the reaction.

Therefore, a new method was designed in order to characterize the average structure in the sample through the reaction. This method showed that the average structure of the cluster grows step-wise, and goes through two stable intermediates before growing to the $\{Bi_{38}O_{45}\}$ cluster. The general reaction is illustrated in Figure 22, where it can be seen that the $[Bi_6O_5(OH)_3(NO_3)_5]\cdot(H_2O)_3$ crystal dissolves directly into an intermediate, which grows until the $\{Bi_{38}O_{45}\}$ cluster is reached.

The reaction rate was varied by varying the temperature. At room temperature, the reaction took several days, while at 80°C the reaction took about an hour.

This project is an outstanding improvement of the understanding of "real materials". We have shown that bismuth oxido clusters in solution are affected by temperature and ligands. They are not simply found in one monodisperse phase, but a mixture of phases where the ratio between the phases is constantly changing. Additionally, the phases may exist of size distributions of clusters, where we need new techniques to characterize a unique structure through the reaction.

Further work will be done to combine PDF and SAXS in order to unravel the full potential of these techniques. *In situ* SAXS measurements are currently in progress, which would greatly contribute to the understanding of the cluster growth of bismuth oxido clusters, and other similar systems as uranium-, cerium- and plutonium oxido clusters.

Acknowledgements

Andy Sode Anker acknowledges economic support from Danscatt and economic support and supervision by Kirsten. M. Ø. Jensen and the Nanostructure Group at University of Copenhagen.

I acknowledge the Deutsches Elektronen-Synchrotron for the provision of synchrotron radiation facilities at beamline P02.1 and P07. Thanks to Marcus Weber, Troels Lindahl Christiansen, Kirsten. M. Ø. Jensen and Susan Cooper who performed the *in situ* PDF measurements and Jette K. Mathiesen and Kirsten. M. Ø. Jensen for helping with the *ex situ* PDF measurements.

I thank NBI Institute for the use of in-house Small-Angle X-ray Scattering instrument, and a special thanks to Martin Schmiele, who have done the resolution SAXS calculations, helped with the SAXS measurements and with processing the SAXS data.

The Chemistry Coordination group at Technical University of Chemnitz is acknowledged for providing the crystals needed for this project.

A special thanks to Troels Lindahl Christiansen, who begun the project and have established the idea that the crystals dissolve into an intermediate before they become the $\{Bi_{38}O_{45}\}$ cluster, without seeing an octahedral building block of $\{Bi_6O_X\}$ in solution. He also saw that the ligand exchange stabilizes the $\{Bi_{38}O_{45}\}$ structure. Furthermore, he has a major creative role in the project in order to combine traditional and state-of-art methods.

Notes and references

*Address: Nano-Science Center & Department of Chemistry, University of Copenhagen, Universitetsparken 5, 2100 Copenhagen East, Denmark.; *E-mail: Andy@nano.ku.dk*

1. L. Miersch, T. Ruffer, M. Schlesinger, H. Lang and M. Mehring, *Inorg Chem*, 2012, **51**, 9376-9384.
2. F. Y. Du, J. M. Lou, R. Jiang, Z. Z. Fang, X. F. Zhao, Y. Y. Niu, S. Q. Zou, M. M. Zhang, A. H. Gong and C. Y. Wu, *Int J Nanomed*, 2017, **12**, 5973-5992.
3. L. Miersch, T. Ruffer and M. Mehring, *Chem Commun (Camb)*, 2011, **47**, 6353-6355.
4. M. Schlesinger, S. Schulze, M. Hietschold and M. Mehring, *Dalton T*, 2013, **42**, 1047-1056.
5. L. Miersch, T. Rüffer, H. Lang, S. Schulze, M. Hietschold, D. Zahn and M. Mehring, *European Journal of Inorganic Chemistry*, 2010, **2010**, 4763-4769.
6. C. Falaise, C. Volkringer, J. F. Vigier, A. Beaurain, P. Roussel, P. Rabu and T. Loiseau, *Journal of the American Chemical Society*, 2013, **135**, 15678-15681.
7. I. L. Malaestean, A. Ellern, S. Baca and P. Kogerler, *Chem Commun (Camb)*, 2012, **48**, 1499-1501.
8. M. Mehring, in *Clusters – Contemporary Insight in Structure and Bonding*, ed. S. Dehnen, Springer International Publishing, Cham, 2017, DOI: 10.1007/430_2016_4, pp. 201-268.
9. C. Falaise, C. Volkringer, J. F. Vigier, A. Beaurain, P. Roussel, P. Rabu and T. Loiseau, *J Am Chem Soc*, 2013, **135**, 15678-15681.
10. K. J. Mitchell, K. A. Abboud and G. Christou, *Nat Commun*, 2017, **8**, 1445.
11. L. Soderholm, P. M. Almond, S. Skanthakumar, R. E. Wilson and P. C. Burns, *Angew Chem Int Ed Engl*, 2008, **47**, 298-302.
12. K. M. O. Jensen, P. Juhas, M. A. Tofanelli, C. L. Heinecke, G. Vaughan, C. J. Ackerson and S. J. L. Billinge, *Nature Communications*, 2016, **7**.
13. D. Sattler, M. Schlesinger, M. Mehring and C. A. Schalley, *ChemPlusChem*, 2013, **78**, 1005-1014.
14. S. J. L. Billinge and M. G. Kanatzidis, *Chem Commun*, 2004, DOI: 10.1039/b309577k, 749-760.
15. J. K. M. Ø., T. Christoffer, B. Martin and I. B. B., *ChemSusChem*, 2014, **7**, 1594-1611.
16. D. Prill, P. Juhas, S. J. L. Billinge and M. U. Schmidt, *Acta Crystallographica Section A*, 2016, **72**, 62-72.
17. D. Prill, P. Juhas, M. U. Schmidt and S. J. L. Billinge, *Journal of Applied Crystallography*, 2015, **48**, 171-178.
18. T. Li, A. J. Senesi and B. Lee, *Chem Rev*, 2016, **116**, 11128-11180.
19. P. Juhas, C. L. Farrow, X. Yang, K. R. Knox and S. J. Billinge, *Acta Crystallogr A Found Adv*, 2015, **71**, 562-568.
20. C. L. Farrow and S. J. L. Billinge, *Acta Crystallographica Section A*, 2009, **65**, 232-239.
21. D. P., *Annalen der Physik*, 1915, **351**, 809-823.
22. P. Scardi, S. J. L. Billinge, R. Neder and A. Cervellino, *Acta Crystallographica Section A*, 2016, **72**, 589-590.
23. in *Encyclopedia of the Sciences of Learning*, ed. N. M. Seel, Springer US, Boston, MA, 2012, DOI: 10.1007/978-1-4419-1428-6_2276, pp. 2332-2332.
24. C. L. Farrow, P. Juhas, J. W. Liu, D. Bryndin, E. S. Božin, J. Bloch, P. Th and S. J. L. Billinge, *Journal of Physics: Condensed Matter*, 2007, **19**, 335219.
25. P. Juhas, T. Davis, C. L. Farrow and S. J. L. Billinge, *Journal of Applied Crystallography*, 2013, **46**, 560-566.
26. P. J. Xiaohao Yang, Christopher L. Farrow, Simon J. L. Billinge, *xPDFsuite: an end-to-end software solution for high throughput pair distribution function transformation, visualization and analysis, arXiv:1402.3163*.
27. I. Bressler, J. Kohlbrecher and A. F. Thunemann, *Journal of Applied Crystallography*, 2015, **48**, 1587-1598.
28. L. F., *Acta Crystallographica Section B*, 1978, **34**, 3169-3173.
29. M. Dirk, M. Michael and S. Markus, *Angewandte Chemie International Edition*, 2005, **44**, 245-249.
30. M. Michael, M. Dirk, P. Sanna and S. Markus, *Chemistry – A European Journal*, 2006, **12**, 1767-1781.